# Quasi-Classical Trajectory Calculations Analyzing the Reactivity and Dynamics of Asymmetric Stretch Mode Excitations of Methane in the H + $CH_4$ Reaction

**Cipriano Rangel, José C. Corchado, and Joaquín Espinosa-García***

*Departamento de Química Física, Universidad de Extremadura, 06071 Badajoz, Spain*

*Received: May 22, 2006; In Final Form: July 5, 2006*

An exhaustive dynamics study was performed at two collision energies, 1.52 and 2.20 eV, analyzing the effects of the asymmetric ($\nu_3$) stretch mode excitation in the reactivity and dynamics of the gas-phase H + $CH_4$ reaction. Quasi-classical trajectory (QCT) calculations, including corrections to avoid zero-point energy leakage along the trajectories, were performed on an analytical potential energy surface previously developed by our group. First, strong coupling between different vibrational modes in the entry channel was observed, indicating that energy can flow between these modes, and therefore that they do not preserve their adiabatic character along the reaction path; i.e., the reaction is nonadiabatic. Second, we found that the reactant vibrational excitation has a significant influence on the vibrational and rotational product distributions. With respect to the vibrational distribution, our results confirm the purely qualitative experimental evidence, although the theoretical results presented here are also quantitative. The rotational distributions are predictive, because no experimental data have been reported. Third, with respect to the reactivity, we found that the $\nu_3$ mode excitation by one quantum is more reactive than the ground state by a factor of about 2, independently of the collision energy, and in agreement with the experimental measurement of 3.0 ± 1.5. Fourth, the state-to-state angular distributions of the products reproduce the experimental behavior at 1.52 eV, where the $CH_3$ products scatter sideways and backward. At 2.20 eV this experimental information is not available, and therefore the results reported here are again predictive. The satisfactory reproduction of a great variety of experimental data by the present QCT study lends confidence to the potential energy surface constructed by our group and to those results whose accuracy cannot be checked by comparison with experiment.

## I. Introduction

The knowledge obtained in the dynamics studies of atom−diatom triatomic systems is being applied to dynamics studies in polyatomic systems, which are more complex due to the larger number of degrees of freedom involved and to difficulties related to the potential energy surface construction. A subject of great importance is the role played by the reactant vibrational excitations on the reactivity and the dynamics of the reaction, a subject that has focused the attention of a growing number of researchers in recent years due to the development of new experimental techniques and theoretical methods. Thus, the dynamics of vibrationally excited polyatomic reactions presents a challenge both theoretically and experimentally.

Experimentally, the effects of both the reactant stretching and bending excitations have been explored, with pioneering work in this field being carried out by the groups of Zare et al. (see, for instance, refs 1−3 and references therein) and Crim et al. (see, for instance, refs 4 and 5 and references therein).

The reaction of hydrogen with methane and its isotopic analogues is the prototypical gas-phase polyatomic reaction, and it has been widely studied both theoretically and experimentally. The title reaction presents a light−light−heavy mass combination, is practically thermoneutral, and has an appreciable barrier height, 0.56 eV. However, experimentally the state-to-state dynamics study is very difficult at room temperature and low energies, because hot H atoms are produced in the photolysis process, and even in the case of high energies the reaction cross section is still small.[6] Thus, only a few recent experimental dynamics studies are available.[2,6−10] Camden et al.[2] carried out the first experimental study on the effect of the C−H stretch excitation on the gas-phase H + $CH_4$ hydrogen abstraction reaction. They found that at collision energies of 1.52 eV the excitation of the asymmetric C−H stretch mode enhances the reaction cross section by a factor of 3.0 ± 1.5 with respect to the ground-state methane, and that the dominant product channel is stretch-excited $CH_3$, with the ground-state $CH_3$ channel being less important. Moreover, they found that the vibrational excitation has a significant impact on the product state distribution.

In previous theoretical work[11] our group performed a state-to-state dynamics study of the vibrational ground state H + $CD_4$ gas-phase abstraction reaction using quasi-classical trajectory calculations on an analytical potential energy surface (PES) previously developed by our group,[12] named PES-2002. For collision energies in the range 0.7−2.0 eV the HD product rotovibrational distribution agrees with experiment, while the $CD_3$ coproduct appears with a notable internal energy, which has been neither experimentally nor theoretically reported.

To shed more light on the state-to-state dynamics of this reaction, in this paper we describe quasi-classical trajectory (QCT) calculations on the analytical PES-2002 surface to analyze the effect of the methane asymmetric stretch ($\nu_3$) excitation on the reaction cross section, the product vibrational and rotational distributions, and the product scattering distributions, at two collision energies, 1.52 and 2.20 eV, to compare with experimental conditions.

* Corresponding author. E-mail: joaquin@unex.es.

10.1021/jp063118w CCC: $33.50 
Published on Web 08/17/2006

The article is structured as follows: In section II we briefly outline the potential energy surface and the computational assumptions in the QCT calculations. The QCT dynamics results are presented in section III and compared with experimental results. Finally, section IV presents the conclusions.

## II. Potential Energy Surface and Computational Details

**II.A. Potential Energy Surface.** In 2002, our group developed an analytical potential energy surface (PES-2002) to describe the $H + CH_4$ reaction and its isotopic analogues.[12] The PES is wholly symmetric with respect to the permutation of the four hydrogen atoms of methane, and it was calibrated to reproduce thermal rate constants using canonical variational transition-state theory with semiclassical multidimensional tunneling. Since that date, several high-level ab initio calculations have appeared in the literature[13−18] questioning the barrier height. The PES-2002 surface has a barrier height of 12.9 kcal $mol^{-1}$ for the forward reaction, while the most recent high-level ab initio calculations give a substantially higher barrier, $14.8 \pm 0.2$ kcal $mol^{-1}$. Let us analyze these values from a kinetic point of view. On one hand, the PES-2002 reproduces the behavior of the experimental measurements of thermal rate constants and kinetic isotope effects, which are a very sensitive test of different features of the potential energy surface, such as barrier height and width, zero-point energy, and tunneling effect. Moreover, recently Zhao et al.[19] applied the quantum instanton approximation for thermal rate constants to this reaction using our PES-2002. They found that the quantum instanton rates show good agreement with available experimental data over the wide temperature range 200−2000 K and concluded that this result lends support to the accuracy of the present potential energy surface. On the other hand, Pu and Truhlar[16] with a barrier height of 14.8 kcal $mol^{-1}$ obtained good agreement with the available experimental rate constants from 250 to 2400 K using parametrized direct dynamics. However, Wu et al.[14,15] with the same barrier height, 14.8 kcal $mol^{-1}$, and using accurate quantum dynamics calculations found that the theoretical results underestimate the experimental rate constants by a factor of 2−4 over the temperature range 250−500 K. Therefore, it is not only the barrier height, but also the shape of the potential, i.e., the drop toward reactants and products, that will determinate the final result. This is especially true at low temperatures, where tunneling could make the rate constant more dependent on the shape of the PES than on the barrier height. Obviously, in a straight comparison between theory and experiment, the theoretical method used (variational transition-state theory or quantum mechanics method) and the uncertainties associated with experiment will must be taken into account.

Next, let us analyze the reaction from a dynamics point of view. On one hand, it has been recently pointed out that the PES-2002 surface presents some flaws with respect to the calculation of some dynamic properties. So, Camden et al.[7−10] performed theoretical and experimental state-to-state dynamics differential cross sections at high energies (27.8−45.0 kcal $mol^{-1}$) for the $H + CD_4$ reaction. They performed quasi-classical trajectory (QCT) calculations on the PES-2002, finding that the $CD_3$ products are strongly forward scattered, in strong contrast with the experimental evidence, where the $CD_3$ products are sideways−backward scattered with respect to the incident H atom. On the other hand, the PES-2002 surface qualitatively predicts that excitation of the $CH_4$ symmetric stretching and "umbrella" bend modes might be expected to enhance the forward rates, while only the $CH_3$ "umbrella" bend mode can appear vibrationally excited. This qualitative prediction agrees with other quantum scattering calculations.[20−22] Moreover, in previous theoretical work[11] our group performed a state-to-state dynamics study of the vibrational ground state $H + CD_4$ gas-phase abstraction reaction using quasi-classical trajectory calculations on this PES-2002. For collision energies in the range 0.7−2.0 eV, most of the available energy appears as product translational energy, with the HD product being vibrationally and rotationally cold, in agreement with experiment. Experimentally it was found[6] that 9% of the available energy appears as HD rotational energy. Hu et al.[10] used a modest B3LYP surface that gives 20%, while Zhang et al.[13] used an expensive ab initio potential energy surface that gives 17.5%; both theoretical calculations are far from the experimental value. Although Hu et al. proposed that the differences between their theoretical results and experiment are due to experimental problems, and that the conditions from the Valentini et al. CARS experimental study[6] might need to be reinterpreted, our group[11] using the PES-2002 surface obtained values in the range 6−9%, in excellent agreement with experiment. Therefore, although the PES-2002 surface presents some flaws and it shows discrepancies with accurate ab initio barrier heights and experimental product scattering distributions, the reasonable qualitative (and sometimes quantitative) reproduction of a wide variety of kinetic and dynamic experimental data allows us to believe that this analytical surface is well balanced and that most features are reasonably well described. Thus, we believe that it can be used for a broad range of kinetic and dynamic calculations without the need to tailor it for a particular study.

**II.B. Computational Details.** In the present work, quasi-classical trajectory (QCT) calculations[23−25] were carried out using the VENUS96 code,[26] customized to incorporate our analytical PESs. Moreover, two modifications were included to compute the vibrational energy in each normal mode to obtain information on the internal vibrational-energy redistribution (IVR) in the entry channel and the $CH_3$ product vibrational distribution in the exit channel. Since VENUS cannot correctly deal with rotating molecules, to perform this calculation it is necessary to rotate and to translate the molecule so that it matches the reference equilibrium geometry orientation and position that was used to perform the normal-mode analysis. Once this is done, a projection of the displacement and momentum matrices on the normal-mode space allows us to compute the potential and kinetic energy for each normal mode.

To study the IVR in methane, we performed batches of 500 nonreactive trajectories of 2 ps. The initial conditions were set so that we ensured no reaction takes place despite the length of the trajectory. Each set of trajectories was run with excitation of one of the normal modes in methane, and the average energy for each normal mode during the last picosecond was computed for each vibrational state and compared to the average energy obtained from the set of trajectories with no vibrational excitation. The increase in this normal-mode average energy was taken as an indication of the internal flow of energy between normal modes in methane. Note that this energy flow occurs before the collision with the H atom, so that it is not related to the mode−mode coupling along the reaction path (Coriolis-like terms) that we take as a qualitative indication of the energy flow when a reactive collision occurs.

To study the vibrational state of the $CH_3$ coproduct, the energy on each harmonic normal mode was computed for the last geometry on the reactive trajectories. Although since the harmonic approximation was used for this calculation one could

expect a breakdown of the procedure for highly excited states, a similar treatment for the $H_2$ coproduct gave vibrational percentage distributions within 2% of the distribution obtained with more sophisticated methods, namely an inversion of the Rydberg−Klein−Rees approach as implemented in VENUS. Thus, we can assume that this method is accurate enough for our studies.

Finally, in the QCT calculations the integration step was 0.1 fs, with an initial separation between the H atom and methane center of mass of 8.5 Å. For the reactions with vibrationally excited methane, the rotational energy was thermally sampled at 300 K. Two reactant collision energies were considered in the present work, 1.52 and 2.20 eV, and batches of 100 000 trajectories were performed at each energy, with a maximum impact parameter, $b_{max}$, of 1.85 Å.

A serious drawback of the QCT calculations is the question of how to handle the quantum mechanical zero-point-energy (ZPE) problem in the classical mechanics simulation.[27−42] Many strategies have been proposed to correct this quantum dynamical effect (see, for instance, refs 26−34, 39, and 40 and references therein), but no completely satisfactory alternatives have emerged. Here, we employed a histogram binning procedure to analyze the reactive trajectories. However, it has been pointed out that the binning procedure can significantly affect the conclusions of QCT calculations.[43] In an earlier work[44] for the similar Cl + $CH_4$ reaction, five different binning methods were checked. First, we discarded the trajectories with a final value of the vibrational energy below the total ZPE of the products (i.e., the sum of the ZPEs of HCl and $CH_3$), since in the quantum mechanical world this is the lowest limit. This is what we called histogram binning with simple ZPE correction (or HB-ZPE). Second, we tried a more stringent criterion, discarding all trajectories that lead either to an HCl with a vibrational energy below its ZPE or to a $CH_3$ with a vibrational energy below its ZPE. In this way we only count the reactive trajectories for which the nascent $CH_3$ and HCl have vibrational energies above their respective ZPEs. This is what we called histogram binning with double ZPE correction (HB-DZPE). Third, we tested the widely used Gaussian-weighted binning procedure,[43,45] which has the disadvantage that it effectively reduces the number of reactive trajectories (since some trajectories have an almost zero weight) and more trajectories are required to give the same statistical accuracy as the HB-ZPE method.[46] Moreover, we checked the influence of treating the rotational levels; i.e., once we have obtained rational rotational numbers, they are either rounded to the nearest integer or truncated to their integer part (rounded to the lower integer value). This option was checked because systems with a fractional rotational number between 0.5 and 1.0 have a rotational energy below the energy of the first excited state, and in the quantum mechanical world they can only be in the ground state, while the usual histogram binning puts them in the first excited state. Finally, we compared these binning procedures with the simplest method, the widely used histogram binning with no ZPE correction whatsoever. The analysis of the nascent products' rotational distribution showed that,[44] for the vibrationally excited $CH_4$, the histogram binning with double ZPE correction (HB-DZPE) gives better agreement with experiment. Moreover, when the rational rotational numbers ($j'$) were truncated to their integer part (rounded to the lower integer values instead of to the nearest integer), a narrower rotational distribution and better agreement with experiment was obtained. Therefore, in the present work we will also use the HB-DZPE with $j'$ truncated procedure.

## III. Results and Discussion

**III.A. Nomenclature and Coupling of the Normal Modes.** To clarify the nomenclature used in the text, we shall start by describing the vibration normal modes in reactants ($CH_4$) and products ($H_2$ and $CH_3$) obtained with the PES-2002 surface, which closely agree with the experimental data.[12] The methane normal modes are asymmetric stretch ($\nu_3$, 3053 $cm^{-1}$, triply degenerate), symmetric stretch ($\nu_1$, 2887 $cm^{-1}$), torsional bending ($\nu_2$, 1502 $cm^{-1}$, doubly degenerate), and umbrella bending ($\nu_4$, 1340 $cm^{-1}$, triply degenerate). The methyl radical product normal modes are asymmetric stretch ($\nu_3'$, 3180 $cm^{-1}$, doubly degenerate), symmetric stretch ($\nu_1'$, 3010 $cm^{-1}$), deformation bending ($\nu_4'$, 1384 $cm^{-1}$, doubly degenerate), and umbrella bending ($\nu_2'$, 580 $cm^{-1}$). The $H_2$ product stretching mode is 4406 $cm^{-1}$.

In a previous paper[12] for the H + $CH_4$ reaction we found that the methane symmetric stretching mode, $\nu_1$, is coupled to the reaction coordinate and it adiabatically evolves to the $H_2$ stretching mode, while the methane umbrella bending mode, $\nu_4$, adiabatically evolves to the methyl product umbrella mode, $\nu_2'$. In this simple adiabatic picture, the methane asymmetric stretch mode, $\nu_3$, and the torsional bending mode, $\nu_2$, correspond to spectator modes; i.e., they do not change during the reaction. Therefore, this adiabatic model cannot explain the experiment,[2] where the methane triply degenerate asymmetric stretch mode, $\nu_3$, evolves into the $CH_3$ ($\nu_1'$, symmetric stretch) and $CH_3$ ($\nu_2'$, umbrella mode) products.

However, in previous work from our group[47,48] for the similar Cl + $CH_4$ reaction, we found that this simple adiabatic model is incomplete and that coupling between the normal modes is significant, especially in the reactant channel, allowing some energy flow between the normal modes and leading to a nonadiabatic picture. Following this idea, we also performed an exhaustive analysis of the vibrational-mode coupling for the title reaction, H + $CH_4$, using two approaches: first, by calculating the intramolecular vibrational redistribution (IVR) using QCT calculations, and second, by calculating the coupling terms between vibrational modes, $Bmm'$ (Coriolis-like terms),[49] which control the nonadiabatic energy flow between vibrational modes. The first approach can give some information about the energy flow between vibrational modes that takes place in the methane reactant preceding its collision with the H atom. The second approach gives information on the energy flow between the vibrational modes in the complex formed after the collision between the two reactants, which will eventually evolve into the activated complex and then reach the products.

Before the collision between H and $CH_4$ takes place, the $CH_4$ undergoes IVR. According to our classical trajectory calculations, there is an energy flow between modes even in the vibrational ground state (Figure 1, left panel). This flux is mainly from the $\nu_3$ asymmetric stretch to the doubly degenerate $\nu_2$ bending mode. However, quantum mechanically, the energy transferred does not suffice to excite the $\nu_2$ mode, and the molecule remains in its ground state. However, if the $\nu_3$ mode is excited by one quantum (Figure 1, middle panel), the flux of energy to the $\nu_2$ mode could raise it to its first excited state. Thus one could expect that, when a collision takes place, some methane molecules will collide in their $\nu_3 = 1$ state while a fraction of the methane molecules will be in its $\nu_2 = 1$ state. The excitation of $\nu_3$ by two quanta leads to a more complex picture (Figure 1, right panel): the energy in the $\nu_1$ mode is also significant, but since this mode requires a large excitation energy, it is unlikely that the $\nu_1 = 1$ state is significantly populated. However, the $\nu_2$ mode gets enough energy to reach

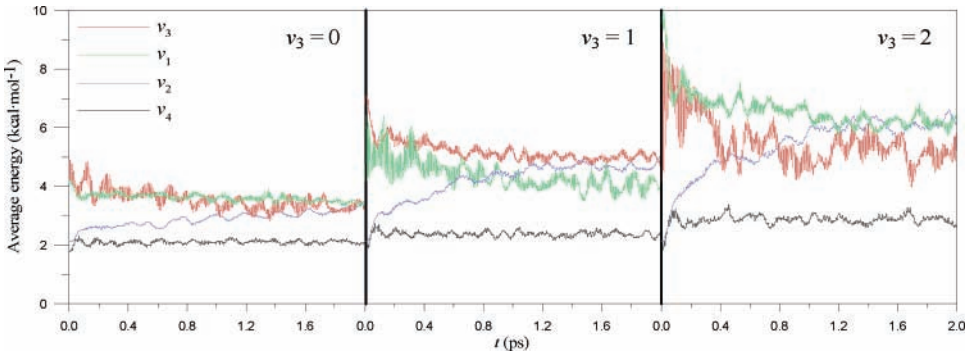


**Figure 1.** Average energy of each normal mode of methane from QCT calculations as a function of time. The left-hand panel shows the results for ground-state methane, the middle panel shows the results for excitation of the asymmetric stretching mode by one quantum, and the right-hand panel shows the results for excitation of the asymmetric stretch by two quanta. The red line shows the average energy of the $\nu_3$ modes, the green line corresponds to the $\nu_1$ mode, the blue line corresponds to $\nu_2$, and the black line corresponds to $\nu_4$.

the first excited state, while the $\nu_3$ mode remains in its first excited state. Thus, when the methane molecule collides with the H atom, there will be a mixture of methane mostly in the $\nu_3 = 1$ plus $\nu_2 = 1$ state, but also in the $\nu_3 = 2$ state, and a small amount of $\nu_3 = 1$ plus $\nu_4 = 1$. Note that this correlation between the classical trajectory results and quantum states is somewhat artificial since, contrary to our classical calculations, in a quantum mechanical world the transfer of infinitesimal amounts of energy is forbidden. Nonetheless, this analysis can help in understanding our QCT results.

Once the reactive collision occurs, the energy flow between modes can be monitored by the coupling terms *Bmm′*. Figure 2 shows the coupling matrix for the nine vibrational modes in methane along the reaction path. In this plot the peaks indicate large coupling between the modes listed on the axes. Hence, in the reactant channel (panel a) we found some degree of coupling between almost all of the modes. Both stretch modes (symmetric and asymmetric) are coupled with the torsional ($\nu_2$) and umbrella ($\nu_4$) bending modes in methane. This coupling is especially important between $\nu_1$ (mode 4) and $\nu_4$ (modes 7, 8, and 9), and between $\nu_2$ (modes 5 and 6) and $\nu_4$ (modes 7, 8, and 9). Therefore, there is significant mode mixing, and the reaction does not preserve vibrational adiabaticity along the reaction path; i.e., the reaction is nonadiabatic.

Note that the degeneracy of some of the modes is broken as the H atom approaches the methane molecule (although the notation of the normal modes in methane is kept for the sake of clarity). However, modes 8 and 9 remain degenerate all along the reaction path, as well as modes 2 and 3 (that become asymmetric stretches in the $CH_3$ product). Mode 7 becomes the umbrella mode in the $CH_3$ product, and mode 4 turns into the $H_2$ stretch. The evolution of these frequencies along the reaction path is shown in Figure 3.

In the product channel, coupling is less relevant (Figure 2, panel b), and mostly indicates some flux of energy between the lowest frequency modes. Since two of these modes eventually become relative motions of the two products with zero frequency at the product asymptote, this flux could be related to rotational or translational excitation of the products, although, because of the small coupling found and the simplicity of this *Bmm′* terms analysis, it cannot shed any light on the rotovibrational population of the products.

In sum, the title reaction is nonadiabatic and we find that in the entry channel the methane bending modes are strongly coupled to each other and with the stretching modes. Therefore, for the title reaction, the vibrational excitation of the asymmetric stretch mode, $CH_4(\nu_3)$, could yield products vibrationally excited in different modes, $CH_3(\nu_1')$ and $CH_3(\nu_2')$, which have been

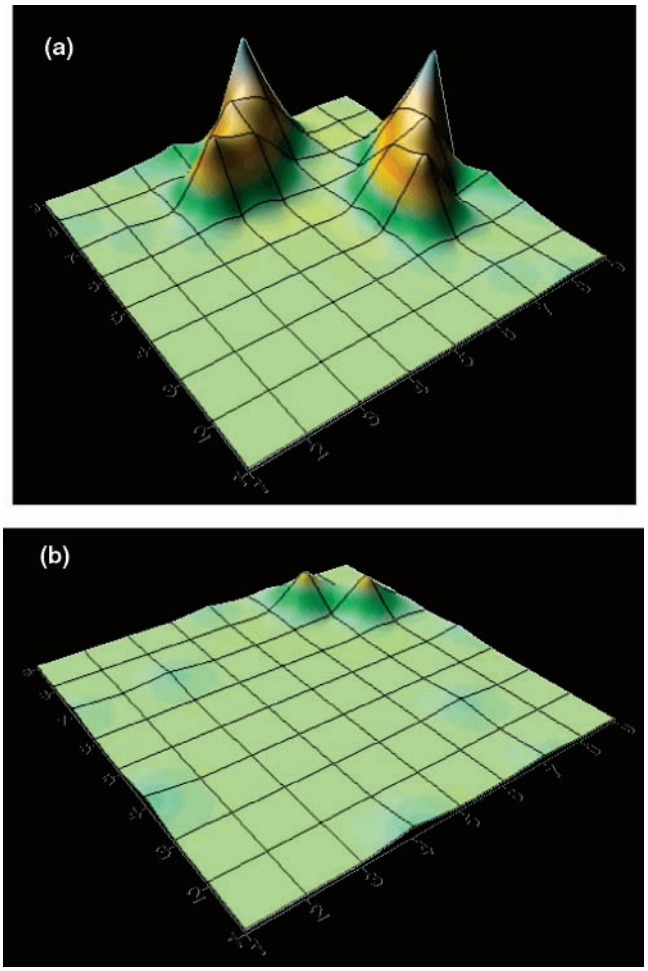


**Figure 2.** Coriolis-like *Bmm′* coupling terms along the reaction path for the nine normal modes in methane. The normal modes are numbered from higher to lower vibrational frequencies. Thus, modes 1, 2, and 3 correspond to $\nu_3$ in methane, mode 4 corresponds to $\nu_1$, modes 5 and 6 correspond to $\nu_2$, and modes 7, 8, and 9 correspond to $\nu_4$. Panel a shows the coupling terms for the reactant channel, while panel b plots the values computed for the product channel. Note that the degeneracy of the modes in methane is broken as the H atom approaches.

experimentally reported,[2] but also in $CH_3(\nu_3')$, doubly degenerate) and $CH_3(\nu_4')$, which have not been experimentally reported for this reaction. Recently, however, Liu et al.,[50] for the $F + CHD_3$ reaction, reported $CD_3$ products excited in the asymmetric stretch, $\nu_3'$, mode.

**III.B. Product Vibrational Distribution.** Table 1 lists the percentage vibrational distributions of the $CH_3$ products for

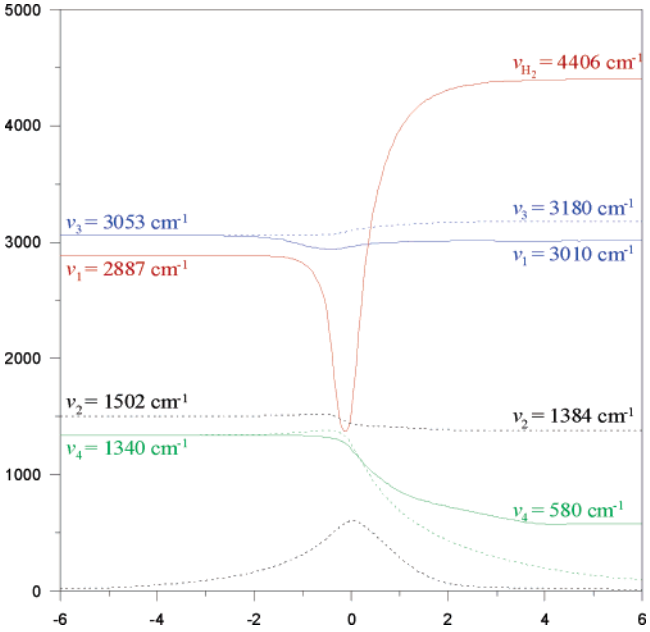


**Figure 3.** Changes in normal-mode frequencies as functions of the reaction coordinate. The dotted lines indicate that two lines are superimposed (i.e., doubly degenerate modes).

different methane vibrational excitations and collision energies. First, we analyze the collision energy effects on the vibrational distribution of $CH_3$ products. For the ground state, $\nu_3 = 1$, and $\nu_3 = 2$ excited methane the vibrational excitation of the $CH_3$ products is independent of the collision energy, 1.52 or 2.20 eV, and practically the same percentages are obtained. Second, we analyze the influence of the methane vibrational excitation on this distribution. The ground-state vibrational methane, at both collision energies, gives mainly ground-state $CH_3$ products. The percentage diminishes with the modes: 62% with excited umbrella bending, 20% with excited deformation bending, and between 2 and 7% in stretching excited modes. This result agrees with the experimental evidence.[2] When the methane asymmetric stretch mode is excited by one quantum, $\nu_3 = 1$, at either collision energy, we find vibrationally hotter $CH_3$ products, especially in the stretching modes, between 15 and 16%. Again, this result agrees with experiment.[2] Finally, when the methane asymmetric stretch mode is excited by two quanta, $\nu_3 = 2$, hotter vibrational $CH_3$ products are obtained, with ≈30% and ≈26% in the $CH_3$ stretch modes, for the collision energies of 1.52 and 2.20 eV, respectively. These theoretical calculations confirm the purely qualitative experimental evidence[2] for the title reaction, indicating that the reactant vibrational excitation has a significant influence on the product state distributions, although the theoretical results here presented also give a quantitative description, absent in experiment.

**III.C. Effect of Vibrational Excitation on the Reactivity.** The QCT total reactive cross sections, $\sigma_R$'s, for the ground-state and the vibrational excited methane ($\nu_3 = 1$ and $\nu_3 = 2$) are listed in Table 2, at two collision energies, 1.52 and 2.20 eV, where all the vibrational states of the products are considered:

$$H + CH_4(\nu) \rightarrow H_2 + CH_3 \qquad (R1)$$

With respect to the ground state, the vibrational excitation of the asymmetric stretch mode by one quantum, $\nu_3 = 1$, enhances the reactivity by a factor of about 2, independently of the collision energy, reproducing the reported experimental factor 3.0 ± 1.5.[2] The excitation of this mode by two quanta, $CH_4$-($\nu_3$=2), enhances the reactivity with respect to the ground state by a factor of about 3, also independently of collision energy. This value was only qualitatively described by experiment,[2] and has never before been calculated.

The relative state-to-state reactive cross sections for the $\nu = 0$, $\nu_3 = 1$, and $\nu_3 = 2$ methane modes are listed in Table 3, at the two collision energies, 1.52 and 2.20 eV, and compared with the available experimental data[2] for the following channels:

$$H + CH_4(\nu{=}0) \rightarrow H_2 + CH_3(\nu{=}0) \qquad (R2a)$$

$$H + CH_4(\nu_3{=}1) \rightarrow H_2 + CH_3(\nu{=}0) \qquad (R2b)$$

$$H + CH_4(\nu_3{=}2) \rightarrow H_2 + CH_3(\nu{=}0) \qquad (R2c)$$

Thus, we define the relative factors F1 and F2 as

$$F1 = \frac{\sigma[H + CH_4(\nu_3{=}1) \rightarrow H_2 + CH_3(\nu{=}0)]}{\sigma[H + CH_4(\nu{=}0) \rightarrow H_2 + CH_3(\nu{=}0)]} \qquad (1)$$

$$F2 = \frac{\sigma[H + CH_4(\nu_3{=}2) \rightarrow H_2 + CH_3(\nu{=}0)]}{\sigma[H + CH_4(\nu{=}0) \rightarrow H_2 + CH_3(\nu{=}0)]} \qquad (2)$$

Experimentally[2] it was found that the F1 factor is always greater than 1 independently of the collision energy; i.e., the methane vibrational excited state $\nu_3 = 1$ enhances the reactivity with respect to the ground state. Our QCT results contrast with experiment, obtaining values F1 < 1. Since our QCT calculations predict that the total cross section increases with the $\nu_3$ excitation (Table 2), this underestimation of the F1 factor seems to suggest that the QCT calculations give $CH_3$ products vibrationally more excited than experiment. With respect to the F2 factor, at 1.52 eV the QCT results agree with experiment; i.e., the reactivity diminishes with respect to the ground state. At 2.20 eV, we find similar behavior, although unfortunately there are no experimental data for comparison.

Table 3 also lists the relative state-to-state cross section for umbrella excited products at the two collision energies, for the following channels:

$$H + CH_4(\nu{=}0) \rightarrow H_2 + CH_3(\nu_2') \qquad (R2d)$$

$$H + CH_4(\nu_3{=}1) \rightarrow H_2 + CH_3(\nu_2') \qquad (R2e)$$

$$H + CH_4(\nu_3{=}2) \rightarrow H_2 + CH_3(\nu_2') \qquad (R2f)$$

Thus, the relative factors F3 and F4 are defined as

$$F3 = \frac{\sigma[H + CH_4(\nu_3{=}1) \rightarrow H_2 + CH_3(\nu_2')]}{\sigma[H + CH_4(\nu{=}0) \rightarrow H_2 + CH_3(\nu_2')]} \qquad (3)$$

$$F4 = \frac{\sigma[H + CH_4(\nu_3{=}2) \rightarrow H_2 + CH_3(\nu_2')]}{\sigma[H + CH_4(\nu{=}0) \rightarrow H_2 + CH_3(\nu_2')]} \qquad (4)$$

For all the umbrella product states there is an enhancement independently of the collision energy, in agreement with experiment.[2] Again, these data were only qualitatively anticipated by experiment, while here we give a quantitative prediction.

Finally, note that the theoretical results presented in this work (Tables 1 and 2) confirm the qualitative experimental data, but also contribute new quantitative information. First, we compared the reactivity of two states, $CH_4(\nu_3{=}2)$ at 1.52 eV and $CH_4$-

**TABLE 1: Percentage Population of $CH_3$ Product Vibrational States**

| | $CH_3$ vibrational state population | | | | | | | | | | | |
|---|---|---|---|---|---|---|---|---|---|---|---|---|
| | $\nu_2'$ | | | $\nu_4'$ | | | $\nu_1'$ | | | $\nu_3'$ | | |
| $CH_4$ vibrational state | 0 | 1 | 2 | 0 | 1 | 2 | 0 | 1 | 2 | 0 | 1 | 2 |
| | | | | | | Collision Energy 1.52 eV | | | | | | |
| gs[a] | 38 | 33 | 29 | 80 | 16 | 4 | 93 | 7 | 0 | 98 | 2 | 0 |
| $\nu_3 = 1$ | 40 | 35 | 25 | 85 | 13 | 2 | 83 | 15 | 2 | 85 | 14 | 1 |
| $\nu_3 = 2$ | 37 | 35 | 28 | 79 | 16 | 5 | 71 | 22 | 7 | 73 | 24 | 3 |
| | | | | | | Collision Energy 2.20 eV | | | | | | |
| gs[a] | 41 | 33 | 26 | 80 | 17 | 3 | 94 | 6 | 0 | 98 | 2 | 0 |
| $\nu_3 = 1$ | 40 | 36 | 24 | 83 | 14 | 3 | 85 | 14 | 1 | 84 | 15 | 1 |
| $\nu_3 = 2$ | 36 | 36 | 28 | 79 | 15 | 6 | 71 | 22 | 7 | 75 | 22 | 3 |

[a] $CH_4$ vibrational ground state ($\nu = 0$).

**TABLE 2: Total Reactive Cross Section ($\sigma_R$[a]) Values and Ratios Between Them**

| | $\sigma_R$ | |
|---|---|---|
| $CH_4$ vibrational state | 1.52 eV | 2.20 eV |
| gs[b] | 0.28 | 0.39 |
| $\nu_3 = 1$ | 0.54 | 0.80 |
| $\nu_3 = 2$ | 0.84 | 1.16 |

| | Ratios Between $\sigma_R$ Values | | | |
|---|---|---|---|---|
| | $\sigma_R(\nu_3=1)/\sigma(\text{gs})$ | | $\sigma_R(\nu_3=2)/\sigma(\text{gs})$ | |
| | 1.52 eV | 2.20 eV | 1.52 eV | 2.20 eV |
| QCT | 1.93 | 2.05 | 3.00 | 2.97 |
| exptl[c] | $3 \pm 1.5$ | | | |

[a] In Å$^2$, with an error bar of $\pm 0.01$. [b] $CH_4$ vibrational ground state ($\nu = 0$). [c] Experimental value from ref 2.

**TABLE 3: State-to-State Reactive Cross Sections[a]**

| | F1 | | F2 | | | |
|---|---|---|---|---|---|---|
| collision energy, eV | QCT | exptl[b] | QCT | exptl[b] | F3 QCT | F4 QCT |
| 1.52 | 0.93 | $\geq 1.4$ | 0.34 | $<1$ | 1.20 | 1.28 |
| 2.20 | 0.78 | $>1$ | 0.46 | | 1.40 | 1.78 |

[a] See text for definition of the F*i* factors. [b] Experimental values from ref 2.

($\nu$=0) at 2.20 eV of collision energy, both with roughly the same total energy. We found that the first is more reactive than the second by a factor of about 2, indicating that vibrational excitation is more effective than a similar amount of energy in translation (Table 2). Moreover, this result corroborates Polanyi's rules for triatomic systems in the case of late transition states. Second, we also confirm the mode selectivity found experimentally. Thus, when the reactions $H + CH_4(\nu_3{=}1)$ at 1.52 and 2.20 eV are compared (Table 1), one finds similar product vibrational state distributions. Similar results are found when two quanta are located in the $\nu_3$ methane mode at 1.52 and 2.20 eV. These results indicate that the initially prepared vibration is more important than the translational energy in determining the product distribution.

**III.D. Effect of Vibrational Excitation on the $H_2$ Product Rotational Distribution.** Because of the large number of product channels opened for the title reaction with these vibrational excitations, $\nu_3 = 1$ and 2, and these collision energies, 1.52 and 2.20 eV, we focused our study on the channels 2a−2c defined above, where all reactions yield the $CH_3$ product in its ground state, and on the following channels:

$$H + CH_4(\nu_3{=}1) \rightarrow H_2(\nu{=}0) + CH_3(\nu_s{=}1) \quad \text{(R2g)}$$

$$H + CH_4(\nu_3{=}2) \rightarrow H_2(\nu{=}0) + CH_3(\nu_s{=}1) \quad \text{(R2h)}$$

where all the reactions yield $CH_3$ products with one quantum in the stretch mode ($\nu_s = 1$). In all the channels analyzed in this section (2a−2c, 2g, 2h), the $H_2$ product is in its ground state. The main aim in this section is to analyze the influence of the vibrational excitation on the $H_2$ product state rotational distribution. The QCT rotational population distributions for $H_2$-($\nu$=0) are plotted in Figures 4 and 5 for the collision energies of 1.52 and 2.20 eV, respectively. Unfortunately, due to experimental difficulties, these rotational distributions are not experimentally known, so that these theoretical calculations are predictive.

At 1.52 eV, in the first set of channels, 2a−2c (three upper panels in Figure 4), where the $CH_3$ product is always in its ground state, one observes that as the methane $\nu_3$ vibrational level becomes more excited the $H_2$ product rotational distribution becomes hotter and broader. Thus the distribution peaks at $j' = 3$, 4, and 6, and extends up to $j' = 9$, 11, and 15, for methane in the states $\nu = 0$, $\nu_3 = 1$, and $\nu_3 = 2$, respectively. In the second set of channels, 2g and 2h (two lower panels in Figure 4), where the $CH_3$ product is excited in the $\nu_s = 1$ state, one observes similar behavior, where the distribution peaks at $j' = 4$ and $j' = 5$, and extends until $j' = 11$ and 13, for the initial methane states $\nu_3 = 1$ and $\nu_3 = 2$, respectively. At 2.20 eV (Figure 5) one finds similar behavior, although the $H_2$ rotational

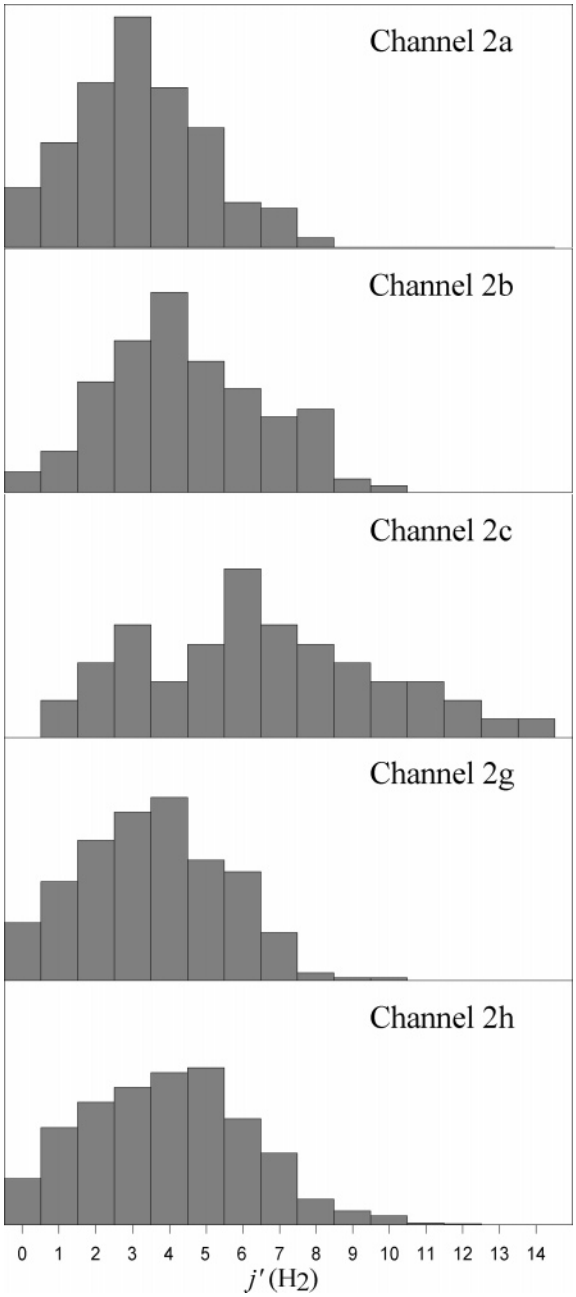


**Figure 4.** Rotational populations of the $H_2$ products at 1.52 eV for channels 2a, 2b, 2c, 2g, and 2h (see text for definition of channels).

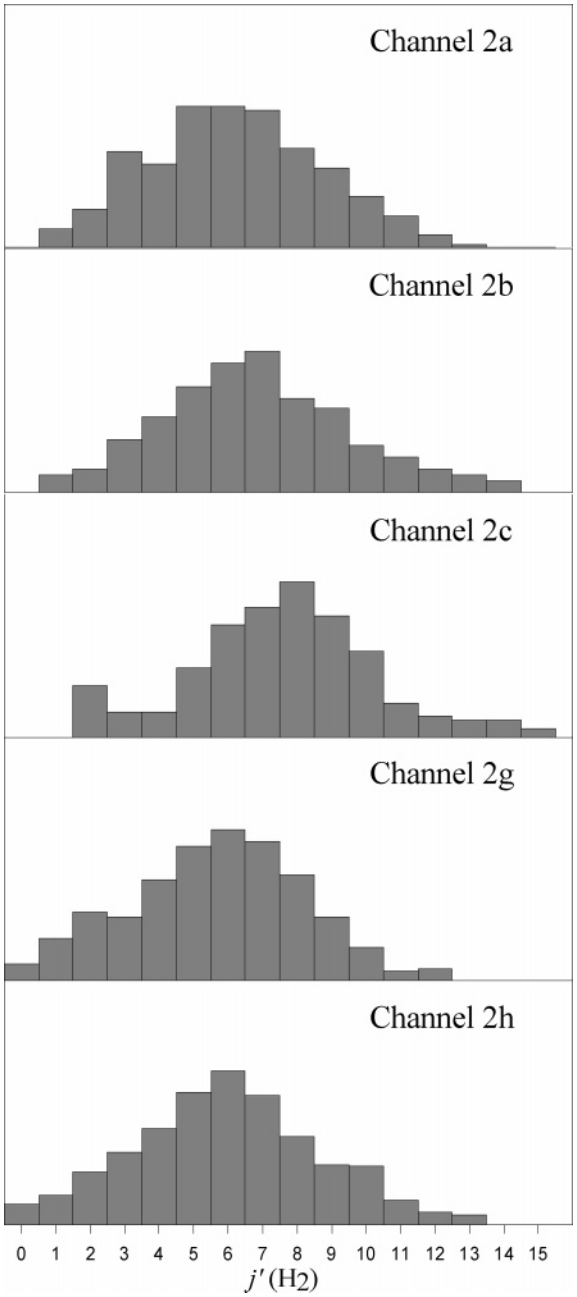


**Figure 5.** Same as Figure 4, but at 2.20 eV.

distributions are slightly hotter (by 1 or 2 units in $j'$) and broader, reaching higher values of $j'$.

**III.E. Effect of Vibrational Excitation on the $CH_3$ Product Scattering Distribution.** With the aim of comparison with the available experimental data, angular distributions in terms of the differential cross section (DCS) for the channels

$$H + CH_4(\nu=0) \rightarrow H_2 + CH_3(\nu=0) \qquad \text{(R2a)}$$

$$H + CH_4(\nu_3=1) \rightarrow H_2 + CH_3(\nu_s=1) \qquad \text{(R2g)}$$

$$H + CH_4(\nu_3=2) \rightarrow H_2 + CH_3(\nu_s=1) \qquad \text{(R2h)}$$

are plotted in Figures 6 and 7 for the collision energies of 1.52 and 2.20 eV, respectively. Note that the only experimental information corresponds to 1.52 eV, while no experimental DCSs at 2.20 eV have been reported. In addition, Figure 8 plots the DCSs for the channel

$$H + CH_4(\nu_3=1) \rightarrow H_2 + CH_3(\nu=0) \qquad \text{(R2b)}$$

at the two collision energies, which have not been experimentally reported.

Experimentally, the scattering distributions were studied only at 1.52 eV, and Camden et al.[2] found that the three first channels (2a, 2g, and 2h) show a similar behavior, where the $CH_3$ products scatter in the sideways and backward directions. The QCT angular distributions reported here (Figure 6) reproduce the experimental evidence. These authors suggested that, since the laboratory-frame speed distributions are similar for the three channels and the 2h channel has more energy, either the products shift more toward backward scattering or more energy is deposited into rotation and vibration of the $H_2$ coproduct. Figure 9 shows a comparison of the experimental and QCT laboratory-

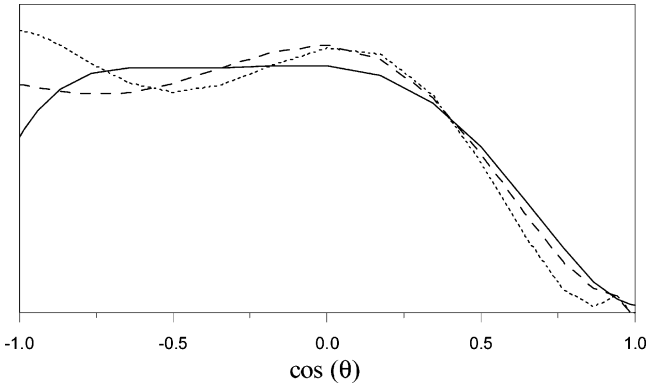


**Figure 6.** Product angular distributions of $CH_3$ products at 1.52 eV for channels 2a (solid line), 2g (dotted line), and 2h (dashed line) (see text for definition of channels). The angular distributions are normalized so that the area under the common regions is the same.

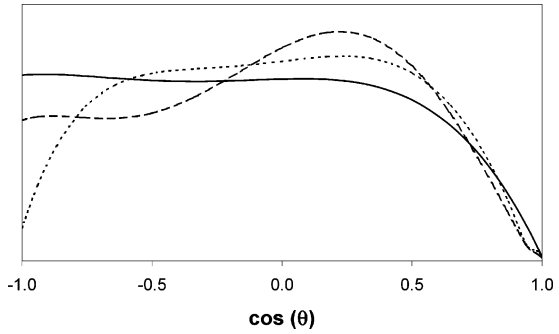


**Figure 7.** Same as Figure 6, but at 2.20 eV.

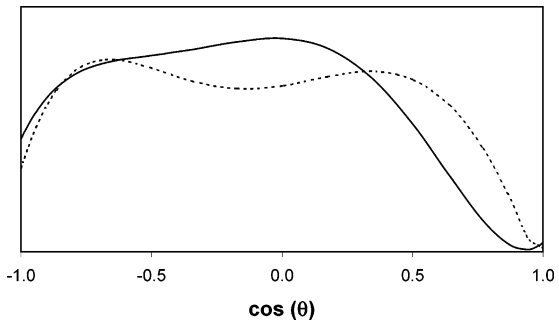


**Figure 8.** Product angular distributions of the $CH_3$ products at 1.52 (solid line) and 2.20 eV (dotted line), for channel 2b.

frame speed distributions. We found similar laboratory-frame speed distributions for the three reactions, in agreement with experiment, although our distributions are narrower and centered at slightly higher values of the $CH_3$ velocity. Our QCT DCSs (Figures 6 and 7) show that reaction R2h does not shift significantly toward the backward hemisphere. Instead, we observed that more energy is deposited in the $H_2$ coproduct: 23% of the total available energy for reactions R2a and R2g and 25% for reaction R2h, although the small differences could also be due simply to statistical errors.

At 2.20 eV, experimental angular distributions are unavailable, and therefore the DCSs plotted in Figure 7 for reactions R2a, R2g, and R2h are predictive, to be confirmed by future experimental measurements. The DCSs are similar to those obtained at 1.52 eV, although the sideways scattering is more pronounced.

Finally, we analyze the DCSs at the two energies for reaction R2b (Figure 8), which have not been measured experimentally.

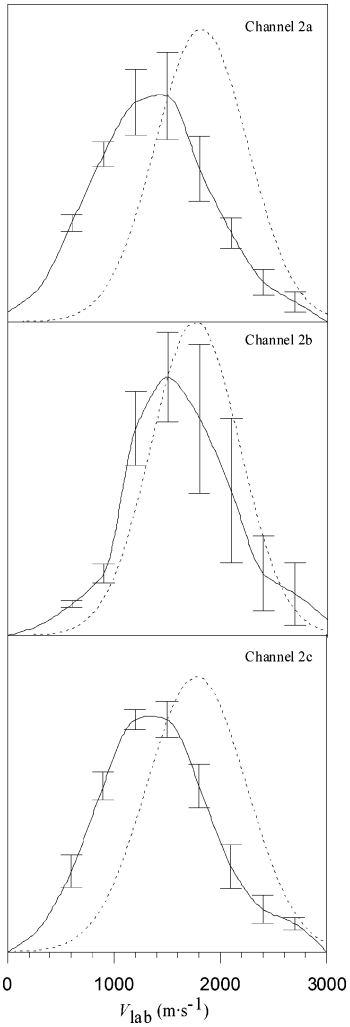


**Figure 9.** Distribution of laboratory-frame speed of $CH_3$ products at 1.52 eV for channels 2a, 2b, and 2c. Solid lines are experimental results from ref 2; dotted lines are from QCT calculations.

The two DCSs are similar, and the $CH_3$ product scatters in the sideways and backward directions, moving toward lower values of the scattering angle as the energy increases. Again, these theoretical calculations are predictive, to be confirmed by future experiments.

## IV. Conclusions

In this paper we have described exhaustive QCT calculations carried out with the aim of analyzing the effect of methane asymmetric vibrational excitations by one and two quanta on the reactivity and dynamics of its reaction with the hydrogen atom. Two collision energies, 1.52 and 2.20 eV, were considered for comparison with experiment. With respect to the reactivity, the main conclusions are the following:

1. Strong coupling between vibrational modes is found, allowing the nonadiabatic flow of energy between modes. Therefore, they do not preserve their adiabatic character along the reaction path; i.e., the reaction is nonadiabatic. This result questions the simple adiabatic picture of located and normal modes.

2. The asymmetric ($\nu_3$) stretch mode excitation by one and two quanta increases the reactivity with respect to the vibrational ground state by factors of $\sim$2 and $\sim$3, respectively, independently of the collision energy. These results agree with the experimental evidence.

ith respect to the dynamics of the excited states, the main conclusions are as follows:

1. As the methane $\nu_3$ vibrational mode gets more excited, hotter vibrational $CH_3$ products are obtained, especially in the stretching excited modes, practically independently of the collision energy. These results confirm the experimental measurements, which indicate that the reactant vibrational excitation has a significant effect on the product state distribution.

2. The $H_2$ product rotational distributions for different state-to-state reactions are mainly dependent on the reactant vibrational excitation and less dependent on the collision energy. These theoretical results are predictive, because unfortunately there is no experimental information for comparison.

3. The methane excited in its asymmetric ($\nu_3$) stretch mode by one and two quanta and the ground-state methane yield similar angular distributions of the products, with the $CH_3$ products scattering sideways and backward. These theoretical results reproduce the known experimental tendency at 1.52 eV. At 2.20 eV similar results were obtained. As experimental information is not available at this energy, these latter results are predictive.

**Acknowledgment.** This work was partially supported by the Junta de Extremadura, Spain (Project No. 2PR04A001).

## References and Notes

(1) Kim, Z. H.; Bechtel, H. A.; Camden, J. P.; Zare, R. N. *J. Chem. Phys.* **2005**, *122*, 084303.
(2) Camden, J. P.; Bechtel, H. A.; Brown, D. J. A.; Zare, R. N. *J. Chem. Phys.* **2005**, *123*, 134301.
(3) Bechtel, H. A.; Camden, J. P.; Brown, D. J. A.; Zare, R. N. *J. Chem. Phys.* **2004**, *120*, 5096.
(4) Yoon, S.; Henton, S.; Zirkovic, A. N.; Crim, F. F. *J. Chem. Phys.* **2002**, *116*, 10744.
(5) Yoon, S.; Holiday, R. J.; Silbert III, E. L.; Crim, F. F. *J. Chem. Phys.* **2003**, *119*, 4755.
(6) Germann, G.; Huh, Y.; Valentini, J. *J. Chem. Phys.* **1992**, *96*, 1957.
(7) Camden, J. P.; Bechtel, H. A.; Zare, R. N. *Angew. Chem., Int. Ed.* **2003**, *42*, 5227.
(8) Camden, J. P.; Bechtel, H. A.; Brown, D. J. A.; Martin, M. R.; Zare, R. N.; Hu, W.; Lendvay, G.; Troya, D.; Schatz, G. C. *J. Am. Chem. Soc.* **2005**, *127*, 11898.
(9) Camden, J. P.; Hu, W.; Bechtel, H. A.; Brown, D. J. A.; Martin, M. R.; Zare, R. N.; Lendvay, G.; Troya, D.; Schatz, G. C. *J. Phys. Chem. A* **2006**, *110*, 677.
(10) Hu, W.; Lendvay, G.; Troya, D.; Schatz, G. C.; Camden, J. P.; Bechtel, H. A.; Brown, D. J. A.; Martin, M. R.; Zare, R. N. *J. Phys. Chem. A* **2006**, *110*, 3017.
(11) Rangel, C.; García-Bernaldez, J. C.; Espinosa-Garcia, J. *Chem. Phys. Lett.* **2006**, *422*, 581.
(12) Espinosa-García, J. *J. Chem. Phys.* **2002**, *116*, 10664.
(13) Zhang, X.; Braams, B. J.; Bowman, J. M. *J. Chem. Phys.* **2006**, *124*, 21104.
(14) Wu, T.; Werner, H.-J.; Manthe, U. *Science* **2004**, *306*, 2227.
(15) Wu, T.; Werner, H.-J.; Manthe, U. *J. Chem. Phys.* **2006**, *124*, 164307.
(16) Pu, J.; Truhlar, D. G. *J. Chem. Phys.* **2002**, *116*, 1468.
(17) Kerkeni, B.; Clary, D. C. *J. Chem. Phys.* **2004**, *120*, 2308.
(18) Yu, H.-G. *Chem. Phys. Lett.* **2000**, *332*, 538.
(19) Zhao, Y.; Yamamoto, T.; Miller, W. H. *J. Chem. Phys.* **2004**, *120*, 3100.
(20) Takayanagi, T. *J. Chem. Phys.* **1996**, *104*, 2237.
(21) Yu, H.-G.; Nyman, G. *J. Chem. Phys.* **1999**, *111*, 3508.
(22) Wang, D.; Bowman, M. *J. Chem. Phys.* **2001**, *115*, 2055.
(23) Porter, R. N.; Raff, L. M. In *Dynamics of Molecular Collisions*; Miller, W. H., Ed.; Plenum Press: New York, 1976; Part B.
(24) Truhlar, D. G.; Muckerman, J. T. In *Atom-molecules Collision Theory*; Bernstein, R. B., Ed.; Plenum Press: New York, 1979.
(25) Raff, L. M.; Thompson, D. L. In *Theory of Chemical Reaction Dynamics*; Baer, M., Ed.; CRC Press: Boca Raton, FL, 1985; Vol. 3.
(26) Hase, W. L.; Duchovic, R. J.; Hu, X.; Komornicki, A.; Lim, K. F.; Lu, D.-h.; Peslherbe, G. H.; Swamy, K. N.; Vande Linde, S. R.;. Varandas, A. J. C.; Wang, H.; Wolf, R. J. VENUS96: A General Chemical Dynamics Computer Program. *QCPE Bull.* **1996**, *16*, 43.
(27) Wu, S. F.; Marcus, R. A. *J. Phys. Chem.* **1970**, *53*, 4026.
(28) Bowman, J. M.; Kuppermann, A. *J. Chem. Phys.* **1973**, *59*, 6524.
(29) Truhlar, D. G. *J. Phys. Chem.* **1979**, *83*, 18.
(30) Schatz, G. C. *J. Chem. Phys.* **1983**, *79*, 5386.
(31) Lu, D.-h.; Hase, W. L. *J. Chem. Phys.* **1988**, *89*, 6723.
(32) Varandas, A. J. C.; Brandao, J.; Pastrana, M. R. *J. Chem. Phys.* **1992**, *96*, 5137.
(33) Varandas, A. J. C.; Marques, J. M. C. *J. Chem. Phys.* **1994**, *100*, 1908.
(34) Varandas, A. J. C. *Chem. Phys. Lett.* **1994**, *225*, 18.
(35) Ben-Nun, M.; Levine, R. D. *J. Chem. Phys.* **1994**, *101*, 8768.
(36) Wang, X.; Ben-Nun, M.; Levine, R. D. *Chem. Phys.* **1995**, *197*, 1.
(37) Ben-Nun, M.; Levine, R. D. *J. Chem. Phys.* **1996**, *105*, 8136.
(38) McCormack, D. A.; Lim, K. F. *Phys. Chem. Chem. Phys.* **1999**, *1*, 1.
(39) Stock, G.; Müller, U. *J. Chem. Phys.* **1999**, *111*, 65.
(40) Müller, U.; Stock, G. *J. Chem. Phys.* **1999**, *111*, 77.
(41) Marques, J. M. C.; Martinez-Nuñez, E.; Fernandez-Ramos, A.; Vazquez, S. *J. Phys. Chem. A* **2005**, *109*, 5415.
(42) Duchovic, R. J.; Parker, M. A. *J. Phys. Chem.* **2005**, *109*, 5883.
(43) Bonnet, L.; Rayez, J. C. *Chem. Phys. Lett.* **1997**, *277*, 183.
(44) Rangel, C.; Navarrete, M.; Corchado, J. C.; Espinosa-Garcia, J. *J. Chem. Phys.* **2006**, *124*, 124306.
(45) Bañares, L.; Aoiz, F. J.; Honvault, P.; Bussery-Honvault, B.; Launay, J.-M. *J. Chem. Phys.* **2003**, *118*, 565.
(46) Xiao, T.; Bowman, J.; Duff, J. W.; Braunstein, M.; Ramachandran, B. J. *Chem. Phys.* **2005**, *122*, 014301.
(47) Sanson, J.; Corchado, J. C.; Rangel, C.; Espinosa-Garcia, J. *J. Chem. Phys.* **2006**, *124*, 074312.
(48) Sanson, J.; Corchado, J. C.; Rangel, C.; Espinosa-Garcia, J. *J. Phys. Chem. A* **2006**, *110*, 9568.
(49) Miller, W. H.; Handy, N. C.; Adams, J. E. *J. Chem. Phys.* **1980**, *72*, 99.
(50) Zhang, B.; Zhang, J.; Liu, K. *J. Chem. Phys.* **2005**, *122*, 104310.